

Performance of various mode indicator functions

M. Radeş*

Universitatea Politehnica Bucureşti, Splaiul Independenţei 313, Bucureşti, Romania

Abstract. Mode Indicator Functions (MIFs) are real-valued frequency-dependent scalars that exhibit local minima or maxima at the modal frequencies of the system. This paper presents an overview of the currently used and some recently developed MIFs, revealing their features and limitations. Eigenvalue or singular value based MIFs use rectangular frequency response function (FRF) matrices calculated in turn at each excitation frequency. Their plots have as many curves as the number of references. Recently developed MIFs do the simultaneous analysis of all FRF information organized in a compound FRF (CFRF) matrix. The left singular vectors or the Q-vectors obtained from the pivoted QLP decomposition of this matrix contain the frequency information and are used to construct MIFs. The number of curves in such a MIF plot is equal to the effective rank of the CFRF matrix. If the number of response coordinates is larger than this rank, a single point excitation can locate even double modes. The condition to use as many input points as the multiplicity of modal frequencies is no more imposed.

Keywords: MMIF, CMIF, CoMIF, UMIF, QCoMIF, QRMIF

1. MIF basic approaches

Mode Indicator Functions (MIFs) are calculated using FRFs measured at N_o response coordinates, N_i input coordinates ($N_i \leq N_o$) and N_f frequencies. Such data are obtained from either multiple-excitation measurements or multi-reference impact tests. A data set consists of $N \leq N_o \times N_i$ complex FRFs measured at N_f discrete frequencies. The primary basis for the selection of input/output locations is the adequate definition of all modes of interest. MIFs have been used to optimize the location of excitation points, for a given set of response measurement points, imposed by the required spatial resolution of mode shapes. The first single curve MIF was developed by Breitbach in 1973 [1] and the first multi-curve MIF – by Hunt, Vold et al. in 1984 [2].

FRFs can be analyzed either in turn, at each frequency, or simultaneously at all frequencies. In the first case, the data set can be visualized as a 3D matrix consisting of N_f rectangular $N_o \times N_i$ FRF matrices (Fig. 1). Each horizontal line along the frequency axis represents an H_{pq} FRF measured at a given combination of output/input coordinates. The various MIF versions employ different formulations based on either the singular value decomposition (SVD) of each $\mathbf{H}_{N_o \times N_i}$ matrix or an eigenproblem involving the real and imaginary parts of the $\mathbf{H}(\omega_f)$ matrices. Examples are the MMIF [2], the CMIF [3] and the related MRMIF, ImMIF and ReMIF. There are as many curves in a plot as the number of references. A comparison of the eigenvalue-based MIFs is presented in [4]. Other MIFs that exhibit zero-crossings at the modal frequencies, like the RMIF [4], are noise sensitive, hence not widely used.

Alternatively, the FRF test data can be arranged in a 2D compound FRF (CFRF) matrix $\mathbf{A}_{N_f \times N_o N_i}$ (Fig. 2) encompassing all FRFs. Each column, \mathbf{a}_j , contains an FRF measured at N_f frequencies, for a given combination of the output and input coordinates. Each row contains $N_o \times N_i$ FRF values, all measured at the same frequency. MIFs based on the SVD of the CFRF matrix are plots of its left singular vectors (or combinations of these) versus frequency. Examples are the UMIF [5] and the CoMIF [6]. There are as many curves in a plot as the effective rank of the CFRF matrix. MIFs based on the pivoted QLP decomposition of the CFRF matrix are plots of its orthogonal Q-vectors (or combinations of these) versus frequency. Examples are the QRMIF and the QCoMIF [7]. They are based on projections onto an orthogonal base of the subspace of measured FRFs and outperform the MMIF and CMIF based on reduced or ‘incomplete’ data sets.

*Corresponding author. E-mail: rades@accessmedia.ro.

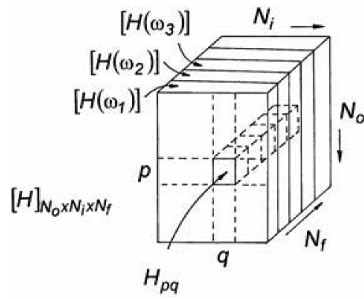


Fig. 1. 3D FRF matrix.

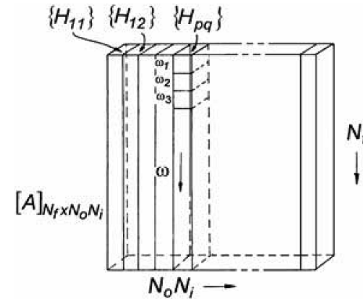


Fig. 2. CFRF matrix.

2. MMIF

For a linear time-invariant structure, at each frequency, the relationship between the complex vector of steady-state response, \mathbf{x} , and the real force vector, \mathbf{f} , is given by

$$\mathbf{x} = \mathbf{x}_R + i \mathbf{x}_I = \mathbf{H}(i\omega) \mathbf{f} = [\mathbf{H}_R(\omega) + i \mathbf{H}_I(\omega)] \mathbf{f}, \quad (1)$$

where $\mathbf{H}_{N_o \times N_i}$ is the dynamic flexibility or the displacement FRF matrix.

The Multivariate Mode Indicator Function (MMIF) is defined [2] by the eigenvalues of the generalized problem

$$\mathbf{H}_R^T \mathbf{H}_R \mathbf{f} = \alpha \left(\mathbf{H}_R^T \mathbf{H}_R + \mathbf{H}_I^T \mathbf{H}_I \right) \mathbf{f}, \quad (2)$$

plotted against frequency. The matrix products in Eq. (2) are of order N_i so that there are as many MMIF curves as driving points. The curve of the smallest eigenvalue exhibits troughs at the undamped natural frequencies (UNFs). The frequencies where more than one curve has a minimum are likely to be expected natural frequencies. Sometimes, not all troughs in the MMIF indicate modes. Apart from cross-eigenvalue effects, antiresonances can produce fallacious troughs. Hence, it is recommended to use the MMIF not on its own but together with other MIFs or with the composite response spectrum to confirm the validity of its minima.

3. CMIF

The economical SVD of the FRF matrix at each spectral line is defined as

$$\mathbf{H}_{N_o \times N_i} = \mathbf{U}_{N_o \times N_i} \mathbf{\Sigma}_{N_i \times N_i} \mathbf{V}_{N_i \times N_i}^H, \quad (3)$$

where $\mathbf{\Sigma}$ is the diagonal matrix of singular values, \mathbf{U} is the matrix of left singular vectors and \mathbf{V} is the matrix of right singular vectors. Matrices \mathbf{U} and \mathbf{V} have orthonormal columns.

The Complex Mode Indicator Function (CMIF) is defined [3] by the singular values plotted as a function of frequency on a logarithmic magnitude scale. The number of CMIF curves is equal to the number of driving points. The largest singular values have peaks at the damped natural frequencies (DNFs). The frequencies where more than a curve has a peak are likely to be repeated natural frequencies. It is recommended to plot ‘tracked’ CMIFs, connecting points which belong to the same modal vector, instead of ‘sorted’ CMIFs, in which points are connected simply based on magnitude. A detailed review of the CMIF and enhanced FRF concepts is given in [8]. Use of the \mathbf{H}_I matrix instead of \mathbf{H} has some advantages in the location of modes.

The CMIF performance declines for structures with very close frequencies and high damping levels. In such cases, two different curves exhibit flat peaks at very close frequencies which have to be located by cursors. The high damping merges the otherwise distinct close peaks. The MMIF performs better in such cases because it locates the UNFs which are more distant from one another than the corresponding DNFs indicated by the CMIF.

4. UMIF

Using the SVD, the rank N_r of the original CFRF matrix can be determined from the decrease of singular values. The reduced-rank reconstructed CFRF matrix can be expressed as a sum of rank-one principal component matrices [5]

$$\mathbf{A}_{N_f \times N_r} = \sum_{j=1}^{N_r} \sigma_j \mathbf{u}_j \mathbf{v}_j^H \quad (4)$$

The singular values σ_j contain the amplitude information, being a measure of the energy content of the FRF set. The right singular vectors \mathbf{v}_j contain the spatial distribution of energy. The left singular vectors \mathbf{u}_j contain the frequency distribution of energy and are linear combinations of the measured FRFs. Their plot versus frequency is the U-Mode Indicator Function (UMIF) [9]. The UMIF has peaks at the DNFs.

5. CoMIF

The Componentwise Mode Indicator Function (CoMIF) is defined [6] by vectors of the form

$$\mathit{CoMIF}_j = 1 - \mathbf{u}_j \otimes \mathbf{u}_j^*, \quad (5)$$

computed as the difference between a column vector of ones and the element-by-element vector product of the left singular vectors. In Eq. (5) the star superscript denotes the complex conjugate. In the CoMIF plot, the number of curves is equal to the estimated effective rank of the CFRF matrix. Each curve has local minima at the DNFs, with the deepest trough at the natural frequency of the corresponding dominant mode.

6. QCoMIF

The SVD is an orthogonal diagonalization and is expensive to compute for large systems. The QR decomposition is an orthogonal triangularization and is cheaper. Its rank revealing properties can be improved using the pivoted QLP decomposition [10]. Applied to the CFRF matrix, this yields

$$\mathbf{A} = \hat{\mathbf{Q}} \mathbf{L} \hat{\mathbf{P}}^H, \quad \hat{\mathbf{Q}} = \mathbf{Q} \Pi_L, \quad \hat{\mathbf{P}} = \Pi_R \mathbf{P}, \quad (6)$$

where \mathbf{L} is lower triangular, Π_L and Π_R are permutation matrices, $\hat{\mathbf{Q}}$ and $\hat{\mathbf{P}}$ are orthogonal matrices, $\mathbf{P}_{N \times N}$ and $\mathbf{Q}_{N_f \times N}$ have orthonormal columns. The columns of \mathbf{Q} , called Q-Response Functions, are linear combinations of the measured FRFs. They are orthogonal, hence independent, so that the minimization of the norm of the projection onto the complementary orthogonal subspace can be used as a criterion to locate the contributing modes.

The Q-Vector Componentwise Mode Indicator Function (QCoMIF) is defined [7] by vectors of the form

$$\mathit{QCoMIF}_j = \text{diag} (\mathbf{I}_{N_f} - \mathbf{q}_j \mathbf{q}_j^H) = 1 - \mathbf{q}_j \otimes \mathbf{q}_j^*, \quad (7)$$

where \mathbf{q}_j are the columns of \mathbf{Q} and \otimes denotes element-by-element vector product. The QCoMIF has dips at the DNFs. The QCoMIF plot has as many curves as the rank of the CFRF matrix. This is estimated from the decrease of the diagonal elements of the \mathbf{L} matrix. The QCoMIF resembles the CoMIF. The format with subplots of the individual QCoMIFs is often preferred to the format with overlaid curves.

7. Numerical simulation examples

7.1. 5-dof system

Consider the five degrees of freedom (dof) system with non-proportional structural (hysteretic) damping from Fig. 3. Two different FRF data sets (free of noise) will be used in the simulation: case 1 – excitation at points 1, 4

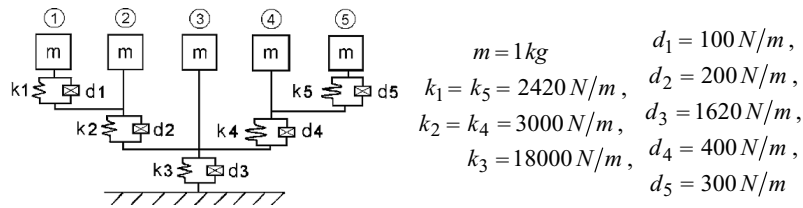


Fig. 3. 5-dof system with hysteretic damping.

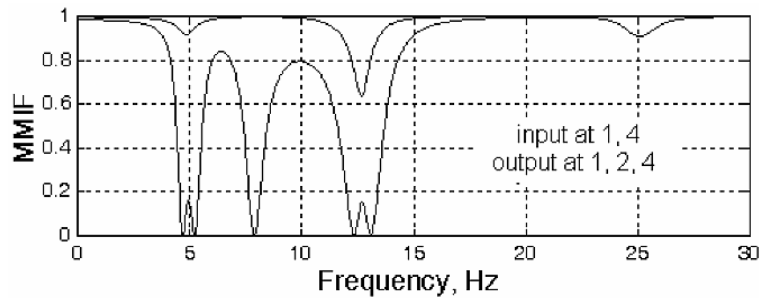


Fig. 4. MMIF for the 5-dof system, case 1.

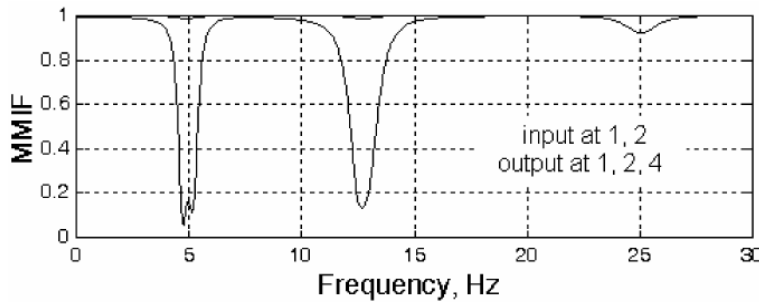


Fig. 5. MMIF for the 5-dof system, case 2.

and response measurement at points 1, 2, 4; case 2 – excitation at 1, 2 and response measurement at 1, 2, 4.

The UNFs are 4.689, 5.213, 12.366, 13.092 and 25.131 Hz. Depending on the FRF data used, the MMIFs can be erroneous indicators. The MMIF plot in Fig. 4 has a fallacious trough at 7.8 Hz, produced by an antiresonance, while the MMIF in Fig. 5 does not indicate all modes.

The DNFs are 4.702, 5.202, 12.449, 13.015 and 25.131 Hz. The CMIF plot in Fig. 6 indicates all five modes and performs better than the MMIF from Fig. 4, but the CMIF in Fig. 7 fails to indicate one mode, having only four peaks. This is due to the particular selection of input points.

The UMIF in Fig. 8 locates all five modes and outperforms the MMIF and CMIF plotted for the same FRF data set (case 2) which failed to locate one mode. Using FRFs from a single input point results in an UMIF plot (Fig. 9) which also locates all 5 modes. The number of curves (five) is equal to the rank of the CFRF matrix.

The CoMIF in Fig. 10 locates all five modes. The QCoMIF is shown in Fig. 11. The deepest trough in each subplot locates a mode of vibration. The number of subplots is equal to the effective rank of the CFRF matrix.

7.2. 11-dof system

Consider the 11-dof system with non-proportional structural (hysteretic) damping shown in Fig. 12. The physical parameters are given in Table 1 [6]. Figures 13 and 14 present the MMIF and CMIF computed for 7×2 FRF

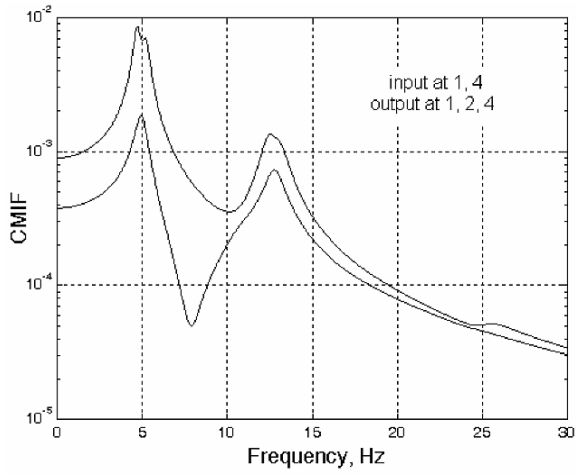


Fig. 6. CMIF for the 5-dof system, case 1.

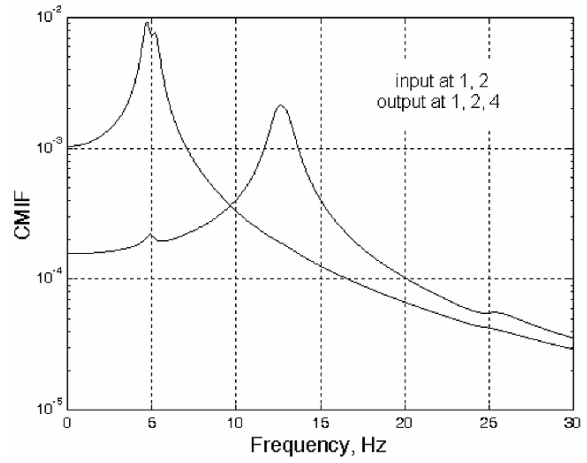


Fig. 7. CMIF for the 5-dof system, case 2.

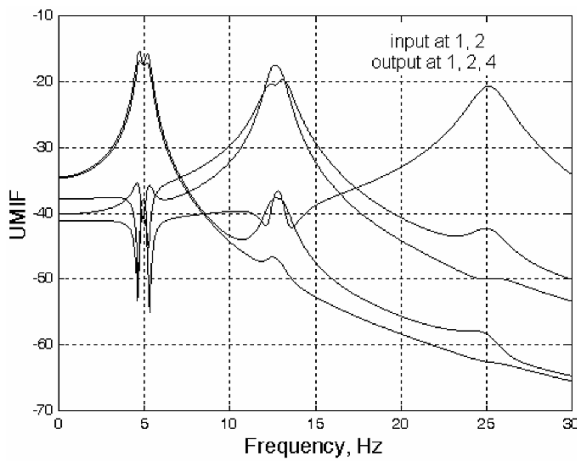


Fig. 8. UMIF for the 5-dof system.

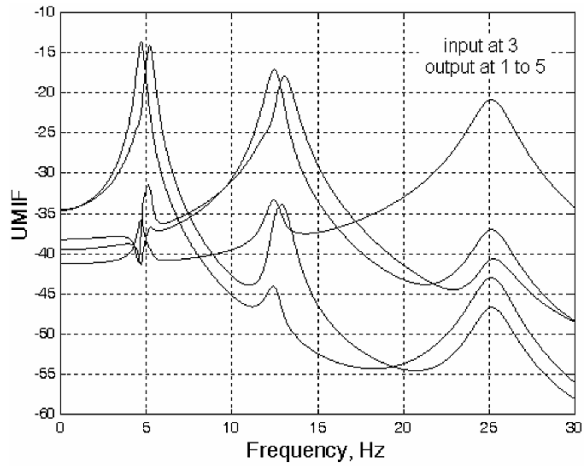


Fig. 9. UMIF for the 5-dof system.

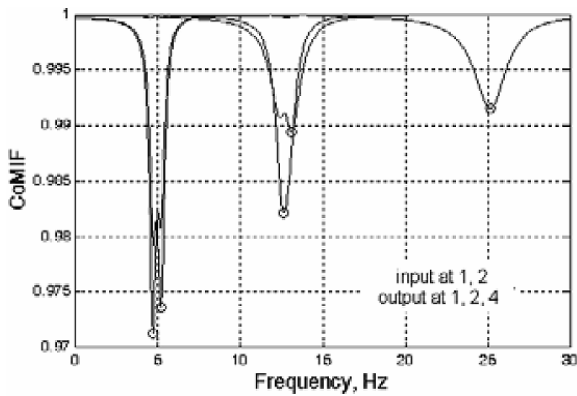


Fig. 10. CoMIF for the 5-dof system.

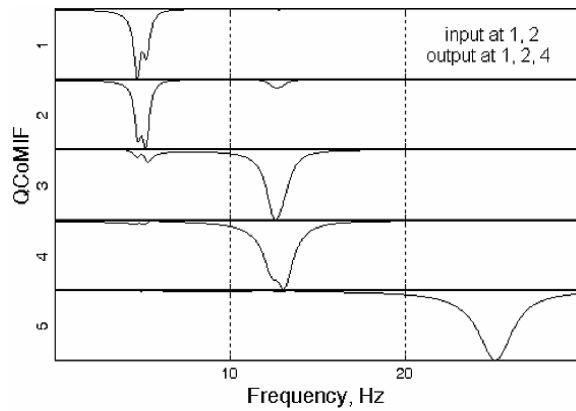


Fig. 11. QCoMIF for the 5-dof system.

Table 1
Physical and modal parameters of the 11-dof system

i	Mass	Stiffness	Structural damping	Natural frequency	Damping factor	Mode r
	m_i kg	k_i N/m	d_i N/m	ω_r Hz	η_r %	
1	1	2421	96.8	2.74	8.93	1
2	1	2989	149.5	2.95	9.05	2
3	1	3691	221.4	7.27	8.86	3
4	1	4556	318.9	7.78	9.12	4
5	1	5625	450.0	11.54	8.77	5
6	1	18000	1620.0	12.08	9.20	6
7	1	5625	562.5	15.12	8.64	7
8	1	4556	501.2	15.51	9.34	8
9	1	3691	442.9	18.54	8.89	9
10	1	2989	388.6	19.27	9.11	10
11	1	2421	339.0	28.58	9.00	11

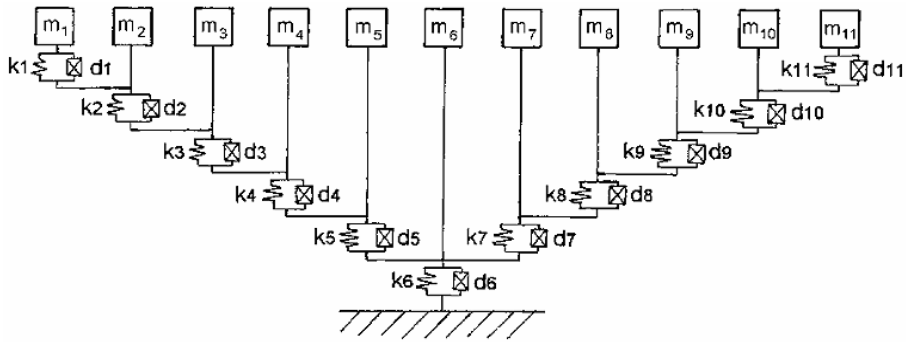


Fig. 12. 11-dof system with hysteretic damping.

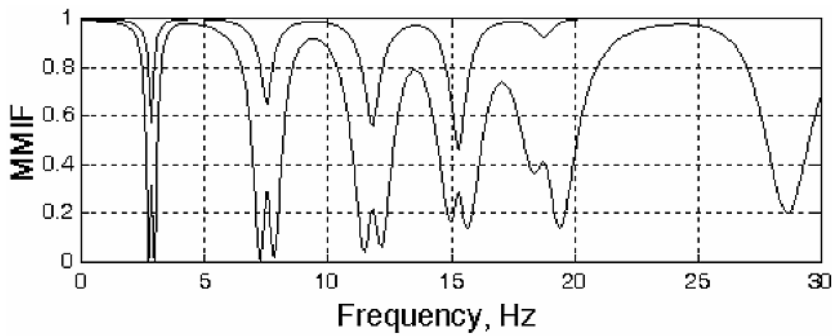


Fig. 13. MMIF for the 11-dof system.

matrices. The MMIF locates 11 modes. The CMIF plot exhibits 6 peaks in the upper curve and 4 peaks in the lower curve, failing to locate one mode.

The peaks in the UMIF from Fig. 15, based on FRFs measured with excitation at only one point, clearly locate all 11 modes. The UMIF from Fig. 16, also locates all 11 modes and can be improved using circles as in Fig. 17.

The CoMIF is given in Fig. 17. The QCoMIF is shown in Fig. 18. The deepest trough in each subplot locates a mode of vibration.

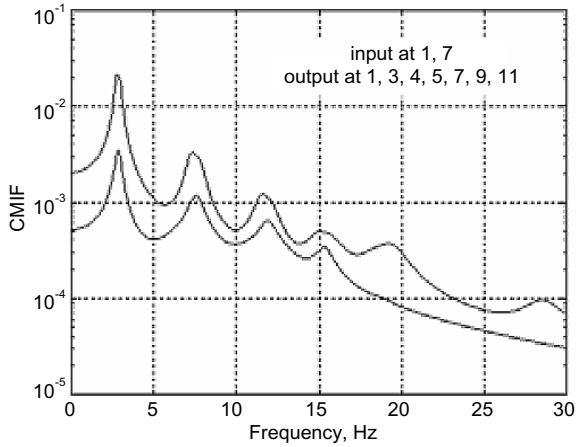


Fig. 14. CMIF for the 11-dof system.

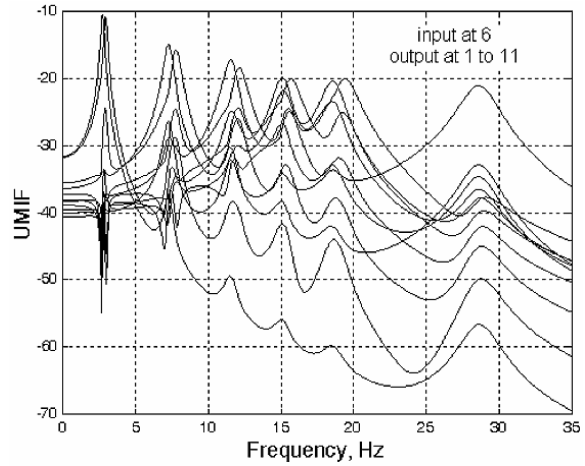


Fig. 15. UMIF for the 11-dof system with one input.

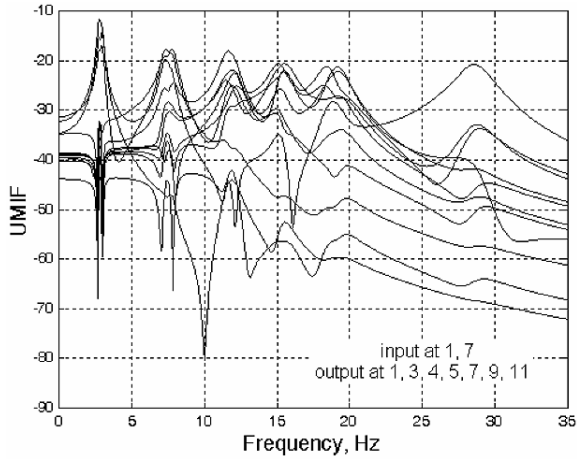


Fig. 16. UMIF for the 11-dof system.

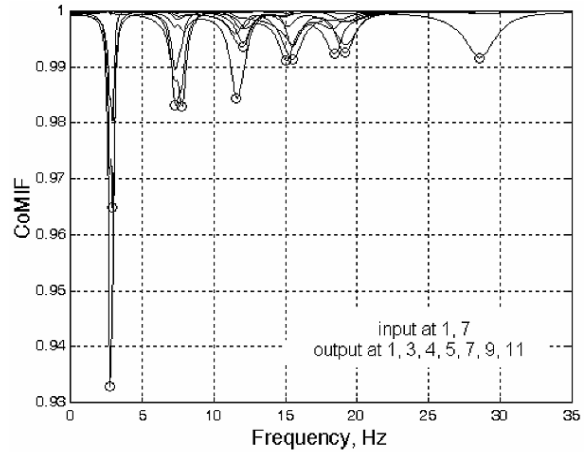


Fig. 17. CoMIF for the 11-dof system.

8. Test data example

The inertance FRFs used in this example were measured on the fan case shown in Fig. 19, in the frequency range 24 to 224 Hz, with 0.25 Hz resolution. Figures 20 and 22 show the CMIF and MMIF calculated based on FRFs from 12 locations (1 to 12 along the lower rim), and 3 force input locations (2, 3 and 50). They detect two pairs of quasi-repeated eigenfrequencies at 103.1 and 177.9 Hz, other dominant modes at 45.75 and 75.7 Hz and some local modes. They perform well for lightly damped structures, but the overlaid MMIF curves should be differently colored to be distinguished from each other.

The ‘complete’ CFRF matrix is of size 801×36 . Figures 21 and 23 show the UMIF and CoMIF based on the first six left singular vectors of a CFRF submatrix, consisting of only the 12 FRFs obtained with excitation at point 50. Each of them consists of six curves and reveals only the six most observable modes of vibration. The QCoMIF in Fig. 24 is based on the first six Q-vectors of the same CFRF submatrix of size 801×12 .

The single curve MIF shown in Fig. 25 is calculated at each frequency as [5]

$$MIF_i = 1 - \frac{\sum_{j=1}^N |\operatorname{Re}(a_{ij})| |a_{ij}|}{\sum_{j=1}^N |a_{ij}|^2}, \quad (8)$$

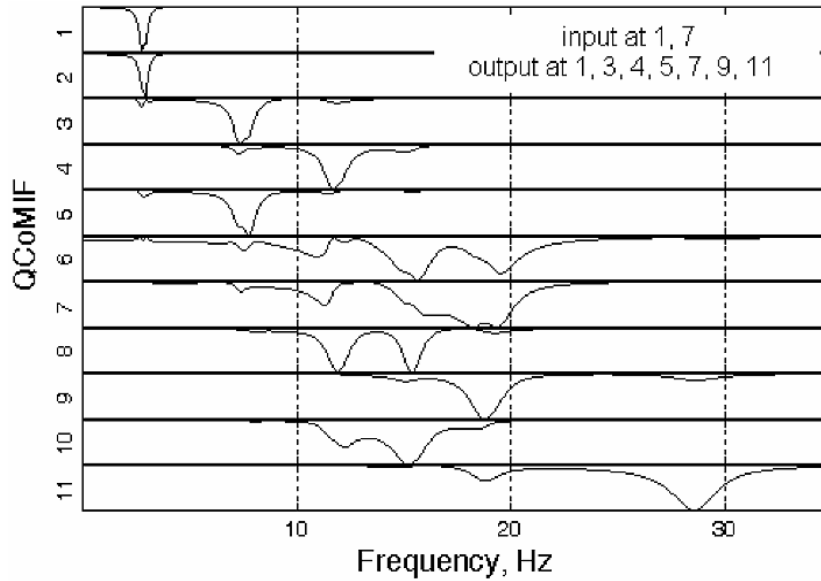


Fig. 18. QCoMIF for the 11-dof system.

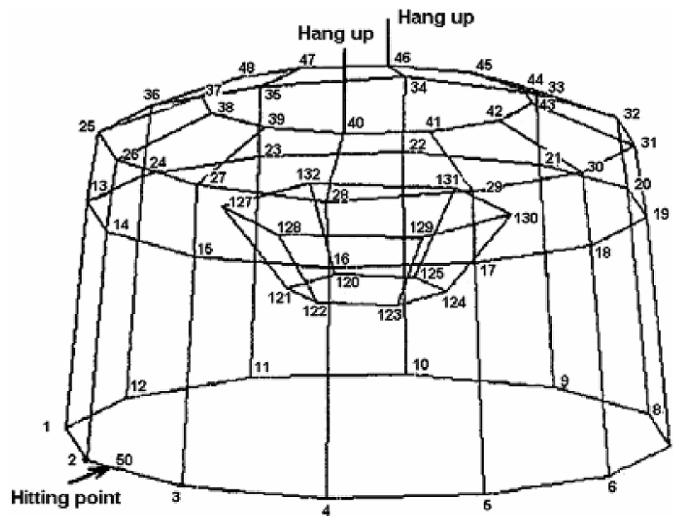


Fig. 19. Test structure.

where the sums extend over the $N = N_o \times N_i = 36$ functions. It locates all modes shown by the CMIF and MMIF except the double modes. A similar MIF is obtained using only the 12 FRFs with excitation at point 50.

9. Concluding remarks

Mode indicator functions are used for the location of observable modes in the test data and their natural frequencies, sometimes together with interference diagrams and singular value ratio plots. Their performance is determined by the selection of input and output locations for the adequate definition of all modes of interest.

The paper outlined some limitations of the traditional MIFs when applied to structures with close frequencies and high damping levels, and the merits of the MIFs based on the principal component analysis. The new MIFs

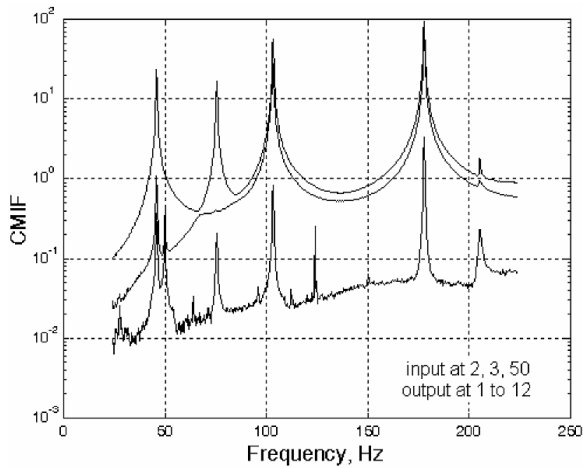


Fig. 20. CMIF for the test structure.

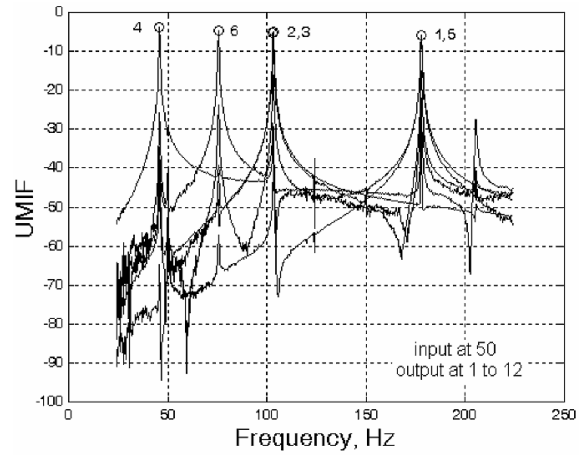


Fig. 21. UMIF for the test structure.

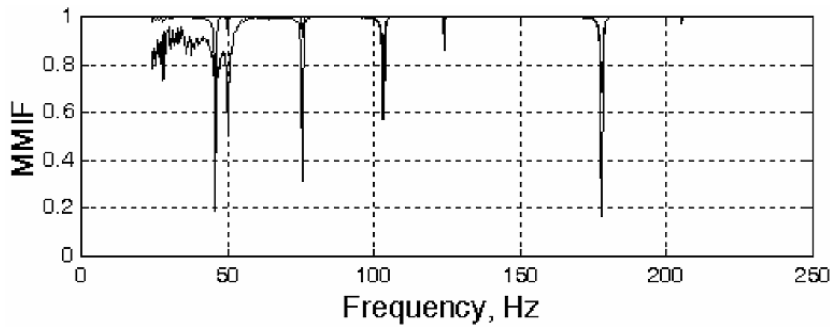


Fig. 22. MMIF for the test structure.

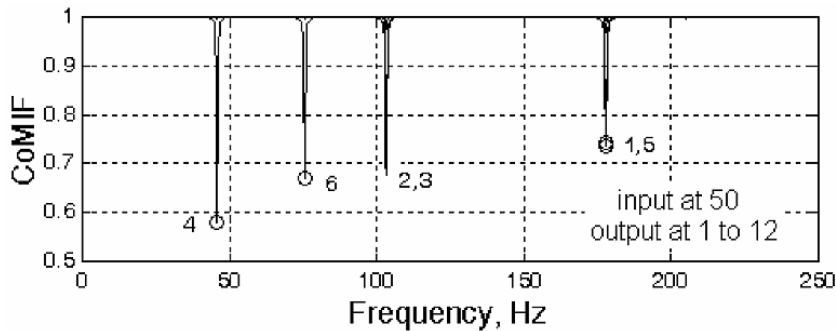


Fig. 23. CoMIF for the test structure.

are computed from orthogonal response functions. These are calculated as linear combinations of the measured FRFs and represent a response dominated by a single mode with a major contribution to the dynamics of the test structure in the given frequency band. MIFs based on principal response functions or on Q-response functions can be calculated from single input excitation data, on condition that the number of response measurement points is larger than the effective rank of the CFRF matrix. The only concern is to avoid the excitation at a nodal point of a mode. The new MIFs perform well for complex structures with high modal density, the number of curves in a plot being limited to the effective rank of the compound FRF matrix.

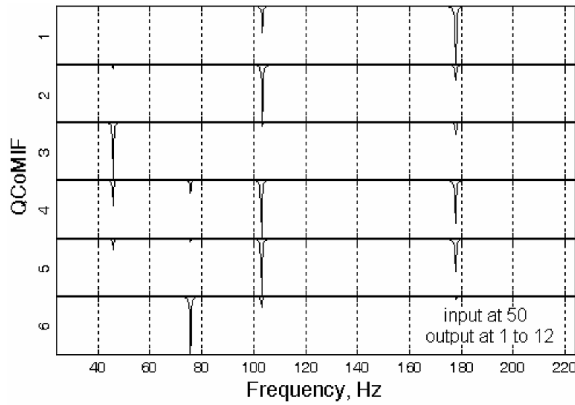


Fig. 24. QCoMIF for the test structure.

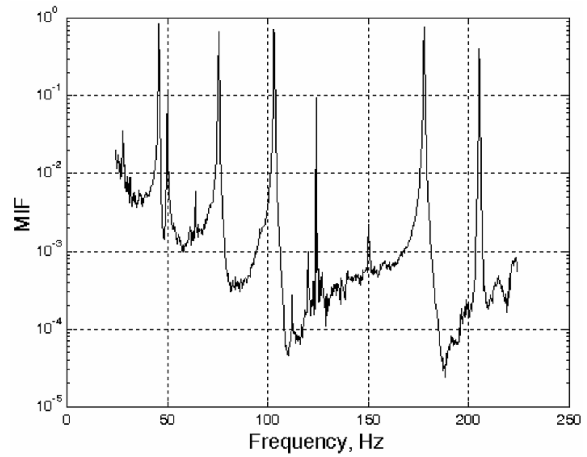


Fig. 25. MIF for the test structure.

References

- [1] E.J. Breitbach, A Semi-Automatic Modal Survey Test Technique for Complex Aircraft and Spacecraft Structures, *Proceedings of 3rd ESA Testing Symposium* (1973), 519–528.
- [2] D.L. Hunt, H. Vold, E.L. Peterson and R. Williams, Optimal Selection of Excitation Methods for Enhanced Modal Testing, *AIAA Paper*, 84–1068, (1984).
- [3] C.Y. Shih, Y.G. Tsuei, R.J. Allemang and D.L. Brown, Complex Mode Indication Function and Its Applications to Spatial Domain Parameter Estimation, *Mechanical Systems and Signal Processing* **2**(4) (1988), 367–377.
- [4] M. Radeş, A Comparison of Some Mode Indicator Functions, *Mechanical Systems and Signal Processing* **8**(4) (1994), 459–474.
- [5] M. Radeş and D.J. Ewins, The Aggregate Mode Indicator Function, *Proceedings of IMAC-XVIII Conference on Structural Dynamics*, San Antonio, Texas, Feb 2000, 201–207.
- [6] M. Radeş and D.J. Ewins, The Componentwise Mode Indicator Function, *Proceedings of IMAC-XIX Conference on Structural Dynamics*, Kissimmee, Florida, Feb 2001, 903–908.
- [7] M. Radeş and D.J. Ewins, MIFs and MACs in Modal Analysis, *Proceedings of IMAC-XX Conference on Structural Dynamics*, Los Angeles, California, Feb 2002, 771–778.
- [8] R.J. Allemang and D.L. Brown, A Complete Review of the Complex Mode Indicator Function (CMIF) with Applications, *Proceedings of ISMA2006 Int. Conference on Noise and Vibration Engineering*, Leuven, Belgium, Sept 2006, 3209–3246.
- [9] M. Radeş, Displays of Vibration Properties, in: *Encyclopedia of Vibration*, (Vol. 1), S.G. Braun, D.J. Ewins and S.S. Rao, eds, Academic Press, London, 2001, pp. 413–431.
- [10] G.W. Stewart, *Matrix Algorithms*, Volume 1: “Basic Decompositions”, SIAM, Philadelphia, 1998.



Hindawi

Submit your manuscripts at
<http://www.hindawi.com>

